

One example of molecular hyperfine structure in the ${}^1\Pi$ state: Study of the $B {}^1\Pi \rightarrow X {}^1\Sigma$ transition of the LuF molecule

C. Effantin, R. Bacis, and J. d'Incan

Laboratoire de Spectrométrie Ionique et Moléculaire, Associé au Centre National de la Recherche Scientifique, 43, boulevard du 11 novembre 1918, 69621-Villeurbanne, France

(Received 28 July 1976)

The accurate measurements obtained with Fabry-Perot spectrometry allowed a detailed determination of the main hyperfine interactions in the (0-0) $B {}^1\Pi \rightarrow X {}^1\Sigma$ transition of the LuF molecule. The corresponding parameters are $Q_{0,0} = -35 \pm 5$ mK, $Q_{1,1} = -30 \pm 4$ mK, $Q_{1,-1} = -34 \pm 3$ mK, $G_{Lu} = 53 \pm 3$ mK, and $G_F \leq 7$ mK. Then it is shown that these parameters give important information on the LuF bond and its origin: high ionicity (> 95%), high c tendency for the excited ${}^1\Pi$ state, probable atomic origin of molecular configurations: $6s6p$ (Lu II) \rightarrow $(6s\sigma)(6p\pi)$ and $6s^2$ (Lu II) \rightarrow $(6s\sigma)^2$.

I. INTRODUCTION

Since the hyperfine effects in the electronic spectrum of HgH were first demonstrated by Mrozowski,¹ numerous diatomic molecules showing a marked hyperfine nuclear structure in some of their electronic transitions have been studied.² It has been seen that interferential spectrometry may constitute a highly accurate method in this study,^{3,4} as well as for measurements on widened absorption lines.⁵⁻⁸ Moreover, this technique may be a useful preliminary investigation device before studies in a lower spectral range with the help of sub-Doppler spectroscopy (saturated absorption, two photon absorption, beam fluorescence, . . .); for instance, when there are large hyperfine interactions (hyperfine components covering a few cm^{-1}) or when it is difficult to obtain the molecule formed at high temperature from a refractory compound. The purpose of this article is to apply this method to the case of the LuF molecule and to define the principal hyperfine interactions for a ${}^1\Pi$ state.

The fine structure of this molecule proves to be extremely regular.⁹⁻¹¹ We chose to study the (0-0) band of the $B {}^1\Pi \rightarrow X {}^1\Sigma$ system the origin of which is situated near 5950 Å; fine structure studies in fact reveal that the excited ${}^1\Pi$ state of this transition could be a pure precession case with a neighboring state $A {}^1\Sigma$. A hyperfine structure should therefore reappear in the molecular excited state close to that of the corresponding configuration of the lutetium.

Moreover, it would be interesting to use the different hyperfine parameters to obtain interesting indications on the structure of the molecule: for instance ionicity of the bond and coupling case of the molecular states.

II. EXPERIMENTAL

The transition was studied by using a Hypeac interferential spectrometer equipped for molecular studies.^{3,4} The source was a composite wall hollow cathode,⁴ the composition of the cathode being 3 Cu atoms per LuF_3 . The double anode lamp is cooled by liquid nitrogen; it runs at intensities varying from 30 to 100 mA. With a Fabry-Perot thickness of 6.5 mm the actual resolving power varies from 600 000 to 450 000 for the lines that are not widened by hyperfine structure. The spectrum studied is located in relation to the fringes of a Fabry-Perot 2 cm in thickness calibrated by using a thorium hollow cathode lamp. The time taken to record 1 cm^{-1} varies from 1 to 6 h.

Figure 1 shows the origin of the R branch; the hyperfine structure of the $R(0)$ line separates it into three well-resolved components of the same width (36 ± 1 mK; $1 \text{ mK} = 0.001 \text{ cm}^{-1}$). Important hyperfine interactions also appear in the $R(1)$ line. A weak branch (marked B in Fig. 1), probably due to a parasitic molecular spectrum, appears near this origin, but since several lines are per-

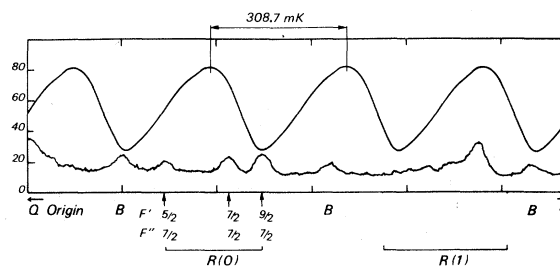


FIG. 1. Origin of the R branch in the (0-0) $B {}^1\Pi \rightarrow X {}^1\Sigma$ transition of the LuF molecule.

fectly separated and well defined it was simple to take this into account, in particular with the $R(3)$ and $R(2)$ lines where superposed. The origin of the Q branch likewise shows a complicated profile (Fig. 2), and even lines of a relatively high quantum number appear to be widened and dissymmetrical (Fig. 3). It should be noted that the spectrographic studies conducted¹⁰ did not enable us to demonstrate any of these effects.

III. THEORY

For a $^1\Sigma$ ground state, the only significant hyperfine interaction is of the electric quadrupolar type; as regards the $^1\Pi$ state, the nuclear spin-electronic orbit interaction should be added.

A. Quadrupolar interaction

This interaction can only come from the lutetium ($I = \frac{7}{2}$) since fluorine has a nuclear spin of $\frac{1}{2}$. The corresponding matrix elements can easily be deduced from the general relations (A1) or (A3) set out in Ref. 3, for instance by taking

$$\langle \Lambda' J' I F' | H_Q | \Lambda J I F \rangle = (-)^{J+I+F+\Lambda'-J'} \delta_{FF'} [(2J+1)(2J'+1)]^{1/2} \left(\frac{(2I+1)(2I+2)(2I+3)}{2I(2I-1)} \right)^{1/2} \times \begin{Bmatrix} J' & J & 2 \\ I & I & F \end{Bmatrix} \begin{pmatrix} J' & 2 & J \\ -\Lambda' & \Lambda' - \Lambda & \Lambda \end{pmatrix} Q_{\Lambda'\Lambda}. \quad (1)$$

This relation corresponds to that given by Freed¹² except for a phase factor. Using the Freed definition, we write

$$Q_{\Lambda'\Lambda} = \frac{1}{4} e Q q_{\Lambda'\Lambda},$$

where e is the proton charge and Q the nuclear quadrupole moment,

$$Q = \langle I, M_I = I | \sum_p 3z_p^2 - r_p^2 | I, M_I = I \rangle,$$

and $q_{\Lambda'\Lambda}$ the electric field gradient coupling constant,

$$\frac{1}{2} q_{\Lambda'\Lambda} = \langle \Lambda' | e_1 \left[\sum_i \frac{C_{\Lambda'-\Lambda}^2(\theta_{iI}, \Phi_{iI})}{r_{iI}^3} - \sum_{p'} \frac{C_{\Lambda'-\Lambda}^2(\theta_{p'I}, \Phi_{p'I})}{r_{p'I}^3} \right] | \Lambda \rangle,$$

where e_1 is the electron charge, the index i corresponding to the electrons, and the index p' to the protons of the other nucleus.

A $^1\Sigma$ state is thus characterized by a single quadrupole coupling constant:

$$Q_{0,0} = \frac{1}{4} e Q q_{0,0}$$

with

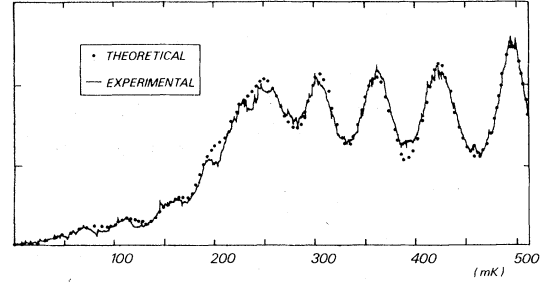


FIG. 2. Theoretical and experimental profiles of the Q head in the $(0-0)$ $B^1\Pi \rightarrow X^1\Sigma$ transition of the LuF molecule.

$S=0$ and $N=J$ in (A3); moreover, it is simple to give a direct demonstration of this (cf. Appendix A). For the electric quadrupole interaction the tensor scalar product defined in Appendix A corresponds to two second-order tensors ($k=2$) (nuclear electric quadrupole moment and electronic orbital field gradient). We thus obtain

$$q_{0,0} = \langle \Lambda' = 0 | e_1 \left(\sum_i \frac{3 \cos^2 \theta_{iI} - 1}{r_{iI}^3} - \frac{2Z}{R^3} \right) | \Lambda = 0 \rangle,$$

where R is the distance between the nuclei and Z the charge of the second nucleus.

In the case of a $^1\Pi$ state, two quadrupole coupling constants are necessary:

$$Q_{1,1} = \frac{1}{4} e Q q_{1,1}, \quad Q_{1,-1} = \frac{1}{4} e Q q_{1,-1},$$

with

$$q_{1,1} = \langle \Lambda' = 1 | e_1 \left(\sum_i \frac{3 \cos^2 \theta_{iI} - 1}{r_{iI}^3} - \frac{2Z}{R^3} \right) | \Lambda = 1 \rangle,$$

$$q_{1,-1} = \langle \Lambda' = 1 | e_1 \sum_i \frac{\sin^2 \theta_{iI} e^{2i\Phi_{iI}}}{r_{iI}^3} | \Lambda = -1 \rangle.$$

Moreover, according to the dependence in Φ_{iI} of those electronic wave functions,¹³ we have $q_{\Lambda'\Lambda} = q_{-\Lambda'-\Lambda}$; hence the diagonal and off-diagonal matrix elements which are present in the $^1\Pi$ state can easily be deduced (Appendix B).

B. Nuclear-spin-electronic-orbit interaction

In the case where the lutetium is the only significant factor, we deduce from formula (A2) in Appendix A by writing $k=1$:

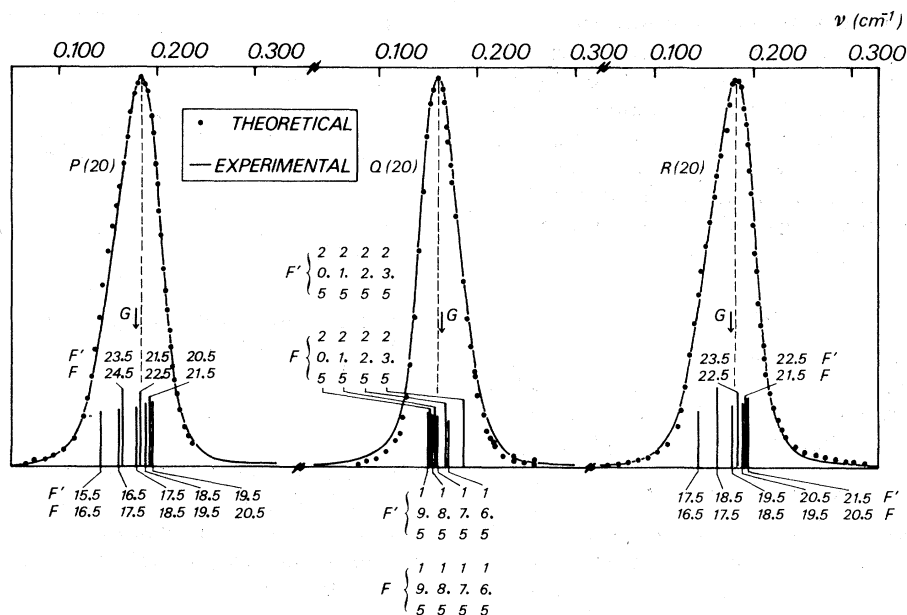


FIG. 3. Theoretical and experimental profiles of $P(20)$, $Q(20)$, and $R(20)$ lines— $(0-0) B^1\Pi \rightarrow X^1\Sigma$ transition of the LuF molecule. The dashed line indicates the axis at the top of the line. G marks the place of the center of gravity of the line. Each hyperfine component is represented by a segment with a height proportional to its intensity.

$$\langle \Lambda' J' I F' | H_{IL} | \Lambda J I F \rangle = (-)^{J+I+F+\Lambda'-J'} \delta_{FF'} [(2J+1)(2J'+1)]^{1/2} [(2I+1)I(I+1)]^{1/2} \begin{Bmatrix} J' & J & I \\ I & I & F \end{Bmatrix} \begin{pmatrix} J' & 1 & J \\ -\Lambda' & \Lambda' - \Lambda & \Lambda \end{pmatrix} G_{\Lambda'\Lambda}, \quad (2)$$

with

$$G_{\Lambda'\Lambda} = g\mu_0 g_I \mu_N \langle \Lambda' | \sum_i \frac{T_{\Lambda'-\Lambda}^1(l_i)}{r_{iI}^3} | \Lambda \rangle.$$

Here again $G_{\Lambda'\Lambda} = G_{-\Lambda', -\Lambda}$.

From this we can deduce the matrix elements present in the $^1\Pi$ states (Appendix B) which are characterized by a simple constant which we will call G_{Lu} .

Although the magnetic moment of fluorine is roughly of the same value as that of lutetium, the influence of the fluorine nucleus is most certainly weaker in the nuclear spin electronic orbit inter-

action. Indeed $\frac{1}{2}$ spin instead of $\frac{7}{2}$ gives seven times lower interval between the $J+I$ and $J-I$ lines (2). Then as a first approximation the fluorine interaction will be considered as a small perturbation on the Lu hyperfine structure. We shall see later that this is an excellent approximation because of the weakness of $\langle 1/r^3 \rangle$ for F in LuF. The basic functions for the corresponding coupling scheme are then denoted by $|\Lambda J I_1 F_1 I_2 F_2 \rangle$ where I_1 and I_2 are, respectively, the nuclear spins of Lu and F.

Then it is easy to calculate the corresponding matrix elements (Appendix C):

$$\langle \Lambda' J' I_1 F_1' I_2 F_2' | H_{IL} | \Lambda J I_1 F_1 I_2 F_2 \rangle = (-)^{2F_1+F_2+I_1+I_2+\Lambda'+1} [(2F_1+1)(2F_1'+1)(2J+1)(2J'+1)(2I_2+1)I_2(I_2+1)]^{1/2} \times \begin{Bmatrix} F_2 & I_2 & F_1' \\ 1 & F_1 & I_2 \end{Bmatrix} \begin{Bmatrix} J' & F_1' & I_1 \\ F_1 & J & 1 \end{Bmatrix} \begin{pmatrix} J' & 1 & J \\ -\Lambda' & \Lambda' - \Lambda & \Lambda \end{pmatrix} G'_{\Lambda'\Lambda}, \quad (3)$$

where $G'_{\Lambda'\Lambda}$ is defined for the fluorine atom in the same way as $G_{\Lambda'\Lambda} = G_{Lu}$ and will be denoted G_F .

C. Intensity

The intensity of an electric dipolar hyperfine transition is obtained from the line strength $S_{F',F}$:

$$S_{F',F} = \sum_{qM_{F'}M_F} |\langle \Lambda' J' I F' M'_{F'} | \mu_q^1 | \Lambda J I F M_F \rangle|^2,$$

$$I_{F',F} \sim (2F+1)(2F'+1)(2J+1)(2J'+1) \begin{Bmatrix} J' & F' & I \\ F & J & 1 \end{Bmatrix}^2 \begin{pmatrix} J' & 1 & J \\ -1 & +1 & 0 \end{pmatrix}^2 \begin{cases} 1 + (-)^{J+J'+1} & \text{for } {}^1\Pi_g \rightarrow {}^1\Sigma^+ \\ 1 - (-)^{J+J'+1} & \text{for } {}^1\Pi_g \rightarrow {}^1\Sigma^+ \end{cases}. \quad (4)$$

It is immediately seen that after summation over F and F' we obtain the usual formula for a ${}^1\Pi \rightarrow {}^1\Sigma^+$ transition.

IV. THEORETICAL RECONSTITUTION OF THE SPECTRUM—DETERMINATION OF CONSTANTS

The experimental spectrum was analyzed from digitized data with readings at equidistant intervals of 3 to 5 mK depending on the total recording time. Since we know the shape of a single line, a theoretical shape can be calculated by working from the previous relations, using an arbitrary set of constants. An attempt is made to minimize the average quadratic difference between each theoretical and experimental point.

A. Method

As fluorine acts only as a small perturbator on the hyperfine structure of lutetium, we turned our attention in the first place to reconstituting the hyperfine structure of the LuF molecule by bringing into play only the structure induced by the lutetium. Four hyperfine parameters were then still to be determined ($Q_{0,0}$ for the ${}^1\Sigma$ state, $Q_{1,1}$, $Q_{+1,-1}$, and G_{Lu} for the excited state).

Before proceeding to systematic trials for the four constants, it is essential to obtain first an idea of their approximate value after a reasonably short space of calculation; to do this, we first ignore all the off-diagonal terms in J . In order to reconstitute the theoretical shape, we determine the shape of a single line; one of the components of $R(0)$ may be chosen, as we have been unable to detect an enlargement of the latter, as will be seen later. Owing to the Doppler temperature of the source, a line from the thorium calibrating spectrum may also be used.

The greatest influence of the hyperfine structure is on the first rotation components. This is why we chose to determine the corresponding parameters by using the $R(0)$ to $R(3)$ lines and the origin of the Q branch, up to and including the $Q(8)$ line.

where μ_q^1 are the components of the irreducible electric dipole moment tensor operator

$$S_{F',F} \sim |\langle \Lambda' J' I F' | | \mu^1 | | \Lambda J I F \rangle|^2.$$

Then the intensity of a hyperfine component for ${}^1\Pi \rightarrow {}^1\Sigma^+$ transition is, after symmetrization of ${}^1\Pi$ wave functions and calculations analogous to the preceding ones,

The $R(0)$ line is made up of three well-resolved components; from the distance between these components G_{Lu} can be determined, as can a linear combination between $Q_{1,1}$ and $Q_{+1,-1}$. A direct check is also made working from the area of the lines recorded to make sure that they are in the ratios (3:4:5) set out in the formula (4), which also enables us to ascribe the corresponding hyperfine transitions without ambiguity (Fig. 1). It was later verified that these ratios are only inappreciably modified when we take the neglected influences into account.

In order to reconstitute the Q branch it is essential to know the distance between the centers of gravity of the rotation lines; we were able to determine it directly by extrapolation from separate Q lines, by interferometrically measuring the position of their center of gravity. The results are in fact the same as these obtained from the values of the rotational constants B' and B'' determined spectrographically.¹⁰

The approximate value of the two remaining parameters may now be determined, by examining the evolution of the rms difference between experimental and theoretical curves with the same aim in view. An intercorrelation test was also used, as well as the weighted sum of the ratios corresponding to the height of the line over difference of heights between experimental and theoretical line; these tests give equivalent results. In this way, the two remaining parameters for each line may be determined, as well as the probable size of errors, working from the different measurements of each line.

It is then possible to evaluate the influence of off-diagonal terms in J by using the four constants determined in this way; we see thus that the $Q(1)$ line must be moved closer to the $Q(2)$ line by 7 mK in relation to the previous ratio and the $R(0)$ line must also be moved closer by 7 mK to the $R(1)$ line. As the positions of the lines are measured interferometrically with a precision of 1 mK, it was possible to verify directly that the

lines recorded were in fact shifted from the expected value; on the other hand, the shift of the higher rotation components could not be shown, as it was lower than 1 mK.

It is also possible to calculate the intensity of the additional lines due to the interaction of the same terms; the intensity of the corresponding branches has been calculated. The only lines which can be observed are found near the R branch, and the most intense line corresponding to this ($J' = 2 \rightarrow J = 0$) has an intensity 50 times lower than that of the $R(0)$ line, so that it is not possible to observe this extra line under optimum conditions of recording. Intensity calculations were therefore carried out without taking into account the nondiagonal interactions in J .

The calculations as a whole lead to the measurements of the parameters indicated in Table I; the rms error indicated corresponds to the dispersion of measurements for each parameter. It is then possible to show that the influence of the fluorine nucleus cannot be demonstrated; this would in fact lead to the doubling or at least to the widening of each component of the $R(0)$ line. By using the relation (3), we can determine the corresponding enlargements. Now, since experimentally the full widths at half maximum (FWHM) of the three components of the $R(0)$ line are equal to within less than 1 mK, it is possible to deduce from this a maximum value for G_F , which is given in Table I.

B. Results

The experimental values obtained in this way from the hyperfine constants defined previously are set out in Table I; the average values of the

TABLE I. Values of the hyperfine parameters and corresponding molecular constants in the $B^1\Pi \rightarrow X^1\Sigma$ transition of the LuF molecule.

$Q_{0,0} = -35 \pm 5$ mK	$\langle (3 \cos^2 \theta - 1) / r^3 \rangle_{1\Pi} = (21 \pm 3) \times 10^{24}$ cm $^{-3}$
$Q_{1,1} = -30 \pm 4$ mK	$\langle (3 \cos^2 \theta - 1) / r^3 \rangle_{1\Pi} = (19 \pm 3) \times 10^{24}$ cm $^{-3}$
$Q_{1,-1} = -34 \pm 3$ mK	$\langle \sin^2 \theta / r^3 \rangle_{1\Pi} = (17 \pm 2) \times 10^{24}$ cm $^{-3}$
$G_{Lu} = 53 \pm 3$ mK	$\langle 1 / r^3 \rangle_{Lu} = 19 \times 10^{25}$ cm $^{-3}$
$G_F \leq 7$ mK	$\langle 1 / r^3 \rangle_F \leq 3 \times 10^{24}$ cm $^{-3}$

molecular parameters deduced from these results are also included in Table I, using for the lutetium nucleus¹⁴

$$Q = 5.6 \times 10^{-24} \text{ cm}^2, \text{ and } \mu_I = 2.0 \mu_N.$$

It should be noted that the fluorine nucleus participates weakly in the gradient of the electric field around the lutetium ($2Z/r^3 \approx 2 \times 10^{24}$ cm $^{-3}$) as compared to the electrons.

In Fig. 2 we have shown the theoretical shape superposed on the experimental shape for the head of the Q branch; we decided against showing the 149 hyperfine components constituting the eight first lines. These components are indicated for the $R(1)$ line (Fig. 4). The differences between the theoretical and experimental shape are sometimes a little greater than might be expected according to the signal-to-noise ratio in the recorded spectra; that may be explained at least partially by the difficulties either in locating the "zero" line or in defining the exact theoretical shape of a single hyperfine component (mainly for far wings). These slight differences did not appear sufficient to warrant the refining of the theoretical model and the measurement of certain

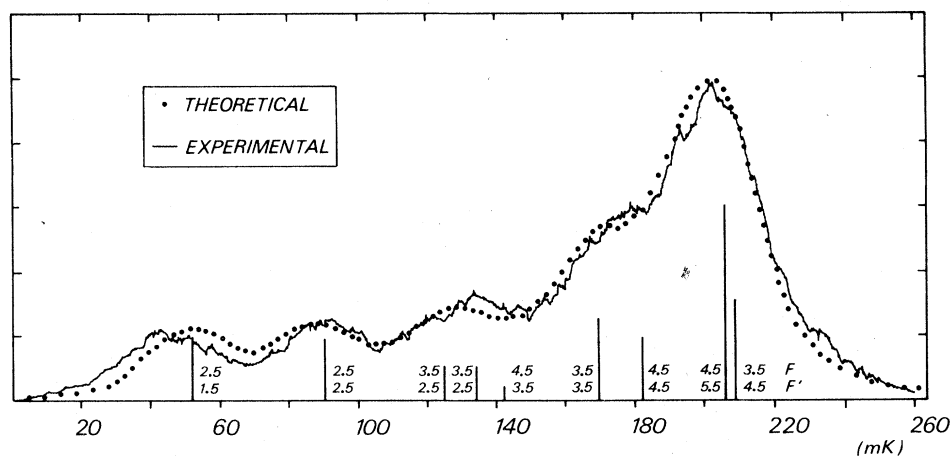


FIG. 4. Theoretical and experimental profiles of $R(1)$ line— $(0-0) B^1\Pi \rightarrow X^1\Sigma$ transition of the LuF molecule. Each hyperfine component is noted by a segment with a height proportional to its intensity.

additional parameters. In spite of this, the control checks were very sensitive to the variations in the parameters used, which explains the value indicated in Table I for the errors.

Figure 3 gives an idea of the precision with which the spectrum has been reconstituted; indeed, the lines considered are distant from those used to determine the parameters; they are recorded with a better signal-to-noise ratio. It is possible to see for instance that the center of gravity G , located in relation to the axis of the top of the line is experimentally defined to within 0.5 mK, and is always theoretically positioned with an error lower than 0.5 mK with respect to its experimental determination.

We see that high-resolution spectrometry by Fabry-Perot is an excellent means of locating the centers of gravity of lines with complex shapes, as has also been shown in the demonstration of low off-diagonal interactions in J .

V. INTERPRETATION AND DISCUSSION

A. Λ doubling

At first sight, the reconstitution of a level of the $^1\Pi$ state might be taken for an abnormal Λ doubling [Fig 5(c) and 5(d)]; in actual fact this is not so, for this doubling is given by the distance between the centers of gravity of the e and f levels that is, 1.2 mK when the level is $J=1$, whatever the types of hyperfine interactions under consideration. In particular, it can be seen in Fig. 5 that the off-diagonal quadrupole coupling in Λ , which seems to produce an abnormal Λ doubling,

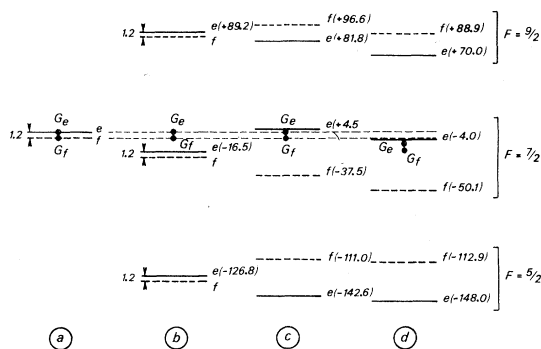


FIG. 5. Hyperfine structure influence on Λ doubling in the $B^1\Pi$ state of LuF , rotational level $J=1$. The relative positions are in mK. G_e and G_f represent the center of gravity of respectively e and f hyperfine levels. (a) e and f Λ doubling components without hyperfine structure, (b) hyperfine components of e and f levels with hyperfine interactions diagonal in Λ , (c) the same as in (b), plus the electric quadrupolar interaction off-diagonal in Λ , (d) the same as in (c), plus interactions off-diagonal in J .

has no influence on the position of the centers of gravity of the e and f levels, which is foreseeable since this separation is due to interaction with external electronic states. The influence of the off-diagonal hyperfine interactions in J on this separation is completely negligible, but they produce a measurable shift of the centers of gravity with relation to their position without these interactions.

B. Hyperfine structure

The hyperfine parameters defined above have a high value which shows that they are induced by the lutetium atom; it is thus logical to try to find out which levels of the lutetium atom could have led to the interactions under study. As regards fluorine, it is only relevant for its ground state $^2P(2s^22p^5)$, as its first excited level $^4P(2s^22p^43s)$ is situated at over $100\,000\text{ cm}^{-1}$.

The first remark that should be made concerns the very low hyperfine interaction with the fluorine nucleus since $\langle 1/r^3 \rangle_{\text{F in LuF}} < 3 \times 10^{24}\text{ cm}^{-3}$. Now, for the ground state of fluorine, from the spin-orbit interaction we find $\langle 1/r^3 \rangle_{\text{F atom}} \approx 44 \times 10^{24}\text{ cm}^{-3}$.¹⁵ This decrease is directly linked to the ionic character of the molecule, given a constitution Lu^+F^- ; the configuration of F^- would be $(2p^6)$

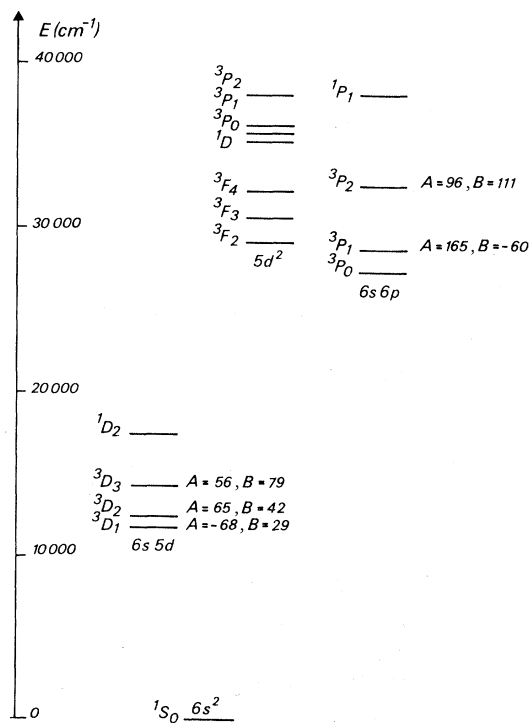


FIG. 6. Low-energy atomic levels of Lu II . The hyperfine parameters A and B are noted in mK from Steudel (Ref. 17).

for which the electric field gradient is very low. It is thus determined that the bond is ionic to over 95%, which is in agreement with the estimation that can be made from the difference in electronegativity of the two elements. We see therefore that the determination of a magnetic hyperfine constant can yield information equivalent to that of the electric quadrupole constants.¹⁶

One is thus led to seek the origin of the molecular transitions starting from the ion Lu^+ . Moreover, it seems preferable to start the discussion with the $^1\Pi$ excited state as the latter supplies more information about the hyperfine structure.

This state most probably originates from the first excited configurations of Lu II: $6s5d$ or $6s6p$ (Fig. 6). We are thus led to consider molecular configurations of the type

$$(\alpha) \dots (5s\sigma)^2(5p\sigma)^2(5p\pi)^4(2p\sigma)^2(2p\pi)^4(6s\sigma)(5d\pi),$$

$$(\beta) \dots (6s\sigma)(6p\pi).$$

It is then possible to obtain information about these configurations by comparing the two quadrupole constants; we may indeed compare them theoretically, like Y. N. Chiu¹⁸: in the case of molecular states with $\Lambda = 1$, where the open-shell configuration is of the type $(\Pi)^0(\sigma)^0$ and of which the other molecular orbitals originate from atomic orbitals with $l \geq 1$, we have

$$q_{1,-1} = \langle \Pi_+^{(0)} | \frac{2C_2^0}{r^3} | \Pi_-^{(0)} \rangle,$$

$$q_{1,1} = \sum_{l=1}^{\infty} \sum_{\Lambda=0}^l \langle \Lambda n l | \frac{2C_2^0}{r^3} | \Lambda n l \rangle.$$

In the latter constant, the contributions originating from all the molecular orbitals of the closed or open shells with $l \geq 1$ are regrouped. In a limited configuration $(\sigma)^0(\Pi)^0$, where $(\Pi)^0$ is the only molecular orbital constructed from an atomic orbital with $l \geq 1$, we write

$$q_{1,-1} = \frac{-\sqrt{6}l(l+1)}{2(3-l^2-l)} q_{1,1},$$

i.e., for a $p\pi$ electron

$$q_{+1,-1} = -\sqrt{6}q_{1,1},$$

then

$$\langle \sin^2\theta/r^3 \rangle_{p\pi} = -2\langle (3\cos^2\theta - 1)/r^3 \rangle_{p\pi}.$$

Now, we find that these two average values, when deduced from the measures of $Q_{1,1}$ and $Q_{-1,1}$ are practically identical; this therefore confirms internal shells contribute to $q_{1,1}$ and explain its relatively high value. We find by difference, that the participation of the core (hypothesis β) is

$$\langle (3\cos^2\theta - 1)/r^3 \rangle_{(1\Pi_\beta)_{\text{core}}} = 27.5 \times 10^{24} \text{ cm}^{-3}.$$

An analogous reasoning for a $d\pi$ electron (hypothesis α) gives

$$\langle \sin^2\theta/r^3 \rangle_{d\pi} = 2\langle (3\cos^2\theta - 1)/r^3 \rangle_{d\pi},$$

which leads to a contribution of $10.5 \times 10^{24} \text{ cm}^{-3}$ for the internal shells.

From these hypotheses we deduce

$$\langle 1/r^3 \rangle_{p\pi} \simeq 20 \times 10^{24} \text{ cm}^{-3},$$

$$\langle 1/r^3 \rangle_{d\pi} \simeq 30 \times 10^{24} \text{ cm}^{-3}.$$

It may be noted that these results are of the same order of magnitude as the corresponding atomic values. In the configuration $(6s5d)$ of Lu II, the simple formula dealing with an electron d gives on the average

$$\langle 1/r^3 \rangle_{\text{Lu II } (6s5d)} \simeq 17 \times 10^{24} \text{ cm}^{-3}.$$

For the configuration $6s6p$, using the Landé interval rule we obtain

$$\langle 1/r^3 \rangle_{\text{Lu II } (6s6p)} \simeq 65 \times 10^{24} \text{ cm}^{-3}.$$

These estimations therefore do not enable us to choose between the two hypotheses under consideration.

Furthermore, the value of $\langle 1/r^3 \rangle$ extracted from the quadrupole parameter $Q_{1,-1}$ should be comparable to that obtained from the magnetic constant G_{Lu} , since in both cases only the unpaired electron intervenes; now the measuring of G_{Lu} leads to $\langle 1/r^3 \rangle \simeq 19 \times 10^{25} \text{ cm}^{-3}$.

This result is approximately ten times greater than that obtained previously using quadrupole interaction; we are therefore obliged to reconsider the physical meaning of the magnetic constant of the $B^1\Pi$ level.

In fact, the calculation of the matrix elements was developed by supposing that the B state was of $^1\Pi$ type in Hund's case (a). It is now necessary to envisage the hypothesis where this state would be governed by the case (c). We would then have a $\Omega = 1$ state for which we could write wave functions of the type¹⁹

$$\begin{aligned} |\alpha, \Omega IF\rangle &= C_\alpha |\alpha, \Lambda \Sigma \Omega IF\rangle \\ &+ \sum_{\alpha''} C_{\alpha''} |\alpha'', \Lambda \pm 1, \Sigma \mp 1, \Omega IF\rangle. \end{aligned}$$

The B state would then originate from a level $^3\Pi$ or $^1\Pi$ ($\Lambda = 1, \Sigma = 0$) combined with $^3\Delta_1$ and $^3\Sigma_1$ states. In this case the matrix elements corresponding to the nuclear-spin-electronic-spin and Fermi interactions are not zero; however, the corresponding angular variations being of the same type as that of the nuclear-spin-electronic-orbit interaction,¹² the magnetic parameter mea-

sured is an effective parameter which encompasses other interactions, which would explain the very high value obtained for $\langle 1/r^3 \rangle$. It may be remarked that a strong tendency towards case (c) of the electronic states of LuF is very likely if we consider the very high values of the spin-orbit constants of the atomic states of Lu I and Lu II.

As regards the $X^1\Sigma$ state, we may envisage correlating it with the configuration $(6s^2)$ of Lu II. For the molecular state we would then have

$$\dots (5s\sigma)^2 (5p\sigma)^2 (5p\pi)^4 (2p\sigma)^2 (2p\pi)^4 (6s\sigma)^2.$$

In this hypothesis, the core alone would contribute to the quadrupole interaction, and we would find

$$\langle (3 \cos^2\theta - 1)/r^3 \rangle_{(1\Sigma)_{\text{core}}} \simeq 21 \times 10^{24} \text{ cm}^{-3},$$

a value comparable to that determined from the $B^1\Pi$ state (hypothesis β).

If we now attempt to make a correlation between the X state and the first excited configuration $6s5d$ of Lu II, we obtain, from the molecular point of view,

$$\dots (6s\sigma) (5d\sigma)$$

by evaluating the contribution of the $d\sigma$ electron with the aid of the value $\langle 1/r^3 \rangle$ obtained from Lu II ($6s5d$) we find

$$\langle (3 \cos^2\theta - 1)/r^3 \rangle_{d\sigma} = 10 \times 10^{24} \text{ cm}^{-3}$$

which leaves a contribution of $11.5 \times 10^{24} \text{ cm}^{-3}$ for the internal shells (value to be compared to that obtained for the $B^1\Pi$ in the hypothesis α).

Therefore, two hypotheses appear to be coherent: (i) X state correlated to the configuration $(6s^2)$ of Lu II and B state correlated to the configuration $(6s6p)$ of Lu II, or (ii) X state and B state correlated to the configuration $(6s5d)$ of Lu II.

However, a fine-structure analysis has demonstrated the presence of a $A^1\Sigma$ state close to the B

state, which seems to be in pure precession with the latter for a value of $L=1$,¹¹ which then would enable the second solution to be eliminated.

VI. CONCLUSION

The accuracy of spectrometrical studies at high resolution by Fabry-Perot interferometry has permitted the precise measurement of the magnetic and quadrupole hyperfine interactions; it was then possible to show that these hyperfine parameters provide interesting information about molecular structure: type of coupling of a state [(a) or (c)], atomic origin of the transitions under consideration, ionic nature of the bond. This transition is situated in an area which is very convenient for study at very high resolution with a cw dye laser; it would therefore be interesting to complete the results obtained in this work by studies conducted, for instance, with the aid of saturated absorption or laser induced fluorescence on a beam.

ACKNOWLEDGMENTS

The help of H. Lefebvre-Brion is gratefully acknowledged, especially for numerous discussions and valuable suggestions about the theory of hyperfine structure and different types of interactions.

APPENDIX A

Let us examine the case of a diatomic-molecule hyperfine Hamiltonian with one coupling nucleus. In this calculation we are dealing with the scalar product of two commuting tensor operators $T^k(Q) \times T^k(L)$ with $k=2$ for the quadrupole interaction and $k=1$ for the nuclear-spin-electronic-orbital interaction [$H_{TL}(1) = \zeta T^1(I) \times T^1(L)/r_{1I}^3$].²⁰ The corresponding matrix elements are when $S=0$, using for instance the relation (7.1.6) in Edmonds,²¹

$$\langle \Lambda' J' I F' M'_F | T^k(Q) \times T^k(L) | \Lambda J I F M_F \rangle = (-)^{J+I+F} \delta_{FF'} \delta_{M_F M'_F} \begin{Bmatrix} F & I & J' \\ k & J & I \end{Bmatrix} \langle \Lambda' J' || T^k(L) || \Lambda J \rangle \langle I || T^k(Q) || I \rangle. \quad (\text{A1})$$

Now the Wigner-Eckart theorem gives

$$\langle \Lambda' J' M' | T_{q'}^k(L) | \Lambda J M \rangle = (-)^{J'-M'} \begin{Bmatrix} J' & k & J \\ -M' & q' & M \end{Bmatrix} \langle \Lambda' J' || T^k(L) || \Lambda J \rangle,$$

where M stands for the z component of J in the laboratory system and $T_{q'}^k(L)$ is a component of $T^k(L)$ in the same system.

The transformation properties of the irreducible

tensor $T^k(L)$ under a rotation of the coordinate system gives

$$T_{q'}^k(L) = \sum_q T_q^k(L) \mathfrak{D}_{q'q}^k(\Phi, \theta, 0),$$

T_q^k being the components with respect to the molecular frame and $\mathfrak{D}_{q'q}^k$ are the matrix elements of finite rotations.

As the basic wave functions of a symmetric top particularized for a diatomic molecule may be

written

$$|v \Lambda JM\rangle = \left(\frac{2J+1}{4\pi} \right)^{1/2} \mathfrak{D}_{\Lambda M}^J(\Phi, \theta, 0) \Psi_{e1, v},$$

we have

$$\begin{aligned} \langle \Lambda' J' M' | T_q^k | \Lambda JM \rangle &= \int \int_{\text{angles}} \sum_q (-)^{\Lambda' - M'} \frac{(2J'+1)^{1/2} (2J+1)^{1/2}}{4\pi} \mathfrak{D}_{-\Lambda' - M'}^J \mathfrak{D}_{q' q}^k \mathfrak{D}_{\Lambda M}^J \langle \Psi_{e1, v} | T_q^k | \Psi_{e1, v} \rangle \sin\theta d\theta d\Phi \\ &= \sum_q (-)^{\Lambda' - M'} (2J'+1)^{1/2} (2J+1)^{1/2} \begin{pmatrix} J' & k & J \\ -\Lambda' & q & \Lambda \end{pmatrix} \begin{pmatrix} J' & k & J \\ -M' & q' & M \end{pmatrix} \langle \Psi'_{e1, v} | T_q^k | \Psi_{e1, v} \rangle \end{aligned}$$

using Eq. (4.6.2) in Ref. 21.

Then

$$\begin{aligned} \langle \Lambda' J' I F' M'_F | T^k(Q) \cdot T^k(L) | \Lambda J I F M_F \rangle &= (-)^{J+I+F+\Lambda'-J'} \delta_{FF'} \delta_{M_F M'_F} (2J+1)^{1/2} (2J'+1)^{1/2} \\ &\times \begin{Bmatrix} F & I & J' \\ k & J & I \end{Bmatrix} \begin{pmatrix} J' & k & J \\ -\Lambda' & \Lambda' - \Lambda & \Lambda \end{pmatrix} \langle I || T^k(Q) || I \rangle \langle \Psi'_{e1, v} | T_q^k(L) | \Psi_{e1, v} \rangle. \end{aligned} \quad (A2)$$

The last two terms are parameters related to nucleus for the first one and electron distribution for the second one.

APPENDIX B

For a $^1\Pi$ state in a symmetrized basis, the wave functions are chosen so that

$$\begin{aligned} |^1\Pi_\phi\rangle &= \frac{1}{\sqrt{2}} (|\Lambda = +1\rangle + |\Lambda = -1\rangle), \\ |^1\Pi_\psi\rangle &= \frac{1}{\sqrt{2}} (|\Lambda = +1\rangle - |\Lambda = -1\rangle). \end{aligned}$$

$$\begin{aligned} \langle ^1\Pi_\phi, J' | H | ^1\Pi_\phi, J \rangle &= \frac{1}{2} [1 + (-)^{J+J'}] (\langle 1, J' | H | 1, J \rangle + \langle -1, J' | H | 1, J \rangle), \\ \langle ^1\Pi_\psi, J' | H | ^1\Pi_\psi, J \rangle &= \frac{1}{2} [1 + (-)^{J+J'}] (\langle 1, J' | H | 1, J \rangle - \langle -1, J' | H | 1, J \rangle), \\ \langle ^1\Pi_\phi J' | H | ^1\Pi_\psi J \rangle &= \frac{1}{2} [1 - (-)^{J+J'}] (\langle 1, J' | H | 1, J \rangle + \langle -1, J' | H | 1, J \rangle). \end{aligned}$$

APPENDIX C

The matrix elements of the nuclear-spin-electronic-orbital interaction in the case of two nuclei with different coupling energies may be written in the following way for the nucleus coupling with the weaker energy

$$\begin{aligned} \langle \Lambda' J' I_1 F'_1 I_2 F'_2 M'_F | T^1(L) \cdot T^1(I_2) | \Lambda J I_1 F_1 I_2 F_2 M_F \rangle \\ = (-)^{2F_1 + F_2 + I_1 + I_2 + J' + 1} \delta_{F'_2 F_2} \delta_{M'_F M_F} [(2F_1 + 1) (2F'_1 + 1)]^{1/2} \begin{Bmatrix} F_2 & I_2 & F'_1 \\ 1 & F_1 & I_2 \end{Bmatrix} \begin{Bmatrix} J' & F'_1 & I_1 \\ F_1 & J & 1 \end{Bmatrix} \\ \times \langle I_2 || T^1(I_2) || I_1 \rangle \langle \Lambda' J' || T^1(L) || \Lambda J \rangle \end{aligned}$$

using Eqs. (7.1.6) and (7.1.7) of Ref. 21, and in the same way as in Appendix A one gets

$$\begin{aligned} \langle \Lambda' J' I_1 F'_1 I_2 F'_2 | T^1(L) \cdot T^1(I_2) | \Lambda J I_1 F_1 I_2 F_2 \rangle \\ = (-)^{2F_1 + F_2 + I_1 + I_2 + \Lambda' + 1} [(2F_1 + 1) (2F'_1 + 1) (2J + 1) (2J' + 1)]^{1/2} \begin{Bmatrix} F_2 & I_2 & F'_1 \\ 1 & F_1 & I_2 \end{Bmatrix} \begin{Bmatrix} J' & F'_1 & I_1 \\ F_1 & J & 1 \end{Bmatrix} \begin{pmatrix} J' & 1 & J \\ -\Lambda' & \Lambda' - \Lambda & \Lambda \end{pmatrix} \\ \times \langle I_2 || T^1(I_2) || I_2 \rangle \langle \Lambda' | T^1_{\Lambda' - \Lambda}(L) | \Lambda \rangle. \end{aligned}$$

Using the relations (1) and (2) it is immediately seen with $H = H_Q$ or H_{IL}

$$\langle 1, J' | H | 1, J \rangle = (-)^{J+J'} \langle -1, J' | H | -1, J \rangle,$$

$$\langle 1, J' | H | -1, J \rangle = (-)^{J+J'} \langle -1, J' | H | +1, J \rangle,$$

when it is noted that $Q_{\Lambda' \Lambda} = Q_{-\Lambda' -\Lambda}$ or $G_{\Lambda' \Lambda} = G_{-\Lambda' -\Lambda}$. Besides these results could be found using symmetry properties of wave functions and Hamiltonian.²²

Then we have

- ¹S. Mrozowski, *Z. Phys.* 72, 776 (1931).
- ²T. M. Dunn, *Molecular Spectroscopy, Modern Research* (Academic, New York, 1972), p. 231.
- ³R. Bacis, R. Collomb, and N. Bessis, *Phys. Rev. A* 8, 2255 (1973).
- ⁴R. Bacis, thesis (University Claude Bernard, 1974) (unpublished).
- ⁵M. Kroll and K. K. Innes, *J. Mol. Spectrosc.* 36, 295 (1970).
- ⁶K. K. Innes, A. Y. Khan, and D. T. Livak, *J. Mol. Spectrosc.* 40, 177 (1971).
- ⁷T. W. Tolbert and K. K. Innes, *J. Am. Chem. Soc.* 95, 7872 (1973).
- ⁸C. D. Olson and K. K. Innes, *J. Chem. Phys.* 64, 2405 (1976).
- ⁹J. D'Incan, C. Effantin, and R. Bacis, *J. Phys. B* 5, L189 (1972).
- ¹⁰C. Effantin, G. Wannous, J. D'Incan, and C. Athenour, *Can. J. Phys.* 54, 279 (1976).
- ¹¹C. Effantin, G. Wannous, and J. D'Incan, *Can. J. Phys.* (to be published).
- ¹²K. Freed, *J. Chem. Phys.* 45, 4214 (1966).
- ¹³See, for instance, B. R. Judd, *Angular Momentum Theory for Diatomic Molecules* (Academic, New York, 1975).
- ¹⁴P. C. Camus, *Gmelins Handbuch der Anorganischen Chemie* (Verlag Chemie, Weirheim, to be published).
- ¹⁵R. G. Barnes and W. V. Smith, *Phys. Rev.* 93, 95 (1954).
- ¹⁶See, for example, the case of chlorine in C. H. Townes and A. L. Schawlow, *Microwave Spectroscopy* (McGraw-Hill, New York, 1955); and W. Gordy and R. L. Cook, *Microwave Molecular Spectra* (Interscience, New York, 1970).
- ¹⁷A. Steudel, *Z. Phys.* 152, 599 (1958).
- ¹⁸Y. N. Chiu, *J. Chem. Phys.* 45, 2990 (1966).
- ¹⁹L. Veseth, *J. Mol. Spectrosc.* 59, 51 (1976).
- ²⁰ $\xi = gg_I\mu_0\mu_N$, where g , g_I , μ_0 , μ_N are the g values for the free electron, the nucleus, Bohr magneton and nuclear magneton, respectively.
- ²¹A. R. Edmonds, *Angular Momentum in Quantum Mechanics* (Princeton U.P., Princeton, N.J., 1957).
- ²²See, for example, J. T. Hougen, NBS Monograph No. 115 (1970) and references therein.